Multiscale-modeling of CNTFETs with non-regular defect pattern

M. Claus*§, D. Teich*, S. Mothes*, G. Seifert** M. Schröter§‡
* Center for Advancing Electronics Dresden, TU Dresden, Germany, martin.claus@tu-dresden.de
§ Chair for Electron Devices and Integrated Circuits, TU Dresden, Germany
** Physical Chemistry, TU Dresden, Germany
‡ ECE Department, UC San Diego, USA,

Introduction

An important consideration in the design and reliability of circuits is the role of defects, impurities, and parameter fluctuations in affecting the transistor characteristics. Here, the impact of vacancies on CNTFET characteristics is studied by means of a multi-scale modeling and simulation framework. Very recently, defect densities of $0.02\,\%$ up to $0.2\,\%$ have been reported for different CNT samples. Therefore and in contrast to other simulation studies [1] at the device level, the impact of defects beyond the single defect limit is analyzed. Our atomistic simulation results suggest the developed defect model at the device level to be a reasonable approach. In addition, it has been shown that in contrast to a single defect, multiple defects lead to a larger variability of the device performance.

Results and Discussion

Atomistic simulations are performed in order to analyze the impact of randomly distributed mono-vacancies for different defect densities. For each defect density, the effective band structure (shown in Fig. 1) is extracted by means of the method described in [2]. The fuzzy shape of the band structure of the defective tube indicates that within a specific energy range, less states are available compared to the number of states for a pristine CNT.

In addition, atomistic CNTFET ($10\,$nm long channel, (14,0)-tube) simulations are performed by means of the recursive Green's function technique described in [3]. Defects are introduced by changing the on-site energies of the p-orbitals. The average impact of randomly distributed defects on the density of states (DOS) and transmission for the reference transistor is shown in Fig. 2. Obviously, defects lead to a cut of the sharp DOS peak as already suggested by the effective band structure shown in Fig. 1.

As expected, with increasing number of defects, the equilibrium transmission spectrum decreases. In Fig. 3, the transmission spectra for two random defect pattern with 5 defects (defect density of $0.4\,\%$) are compared with the average transmission spectra for the same defect density.

For the simulation at the device level, the effective-mass Schrödinger-Poisson solver described in [4] is employed. In order to consider mono-vacancies, randomly distributed distortions of the bandgap along the channel are considered.

Fig. 4 shows a comparison between the pristine DOS and the local DOS averaged along the channel as well as the transmission spectra for different defect densities. The higher the number of local distortions, the stronger is the smoothing of the sharp DOS peak and the lower is the transmission as predicted by the atomistic simulation results shown in Fig. 2.

The impact of defects on the CNTFET behavior is shown in Fig. 6 for 1, 3 and 5 defects. According to Fig. 6 the variations of the on-current I_{on} as well as the threshold voltage V_{th} is larger for a higher number of defects.

Acknowledgment

The authors acknowledge the Cfaed and the DFG projects CL384/2, SCHR95/6 for financial support.

References

[1] N. Neophytou, et al., *APL*, 88(24), 2006.
[2] V. Popescu et al., *PRL*, 10(104), 236403, 2010.
[3] C. Lewenkopf et al., *J. Comp. Elect.*, 12(2), 203–231, 2013.
[4] M. Claus, et al., *J. Comp. Elect.*, 13(2), 689–700, 2014.

ISBN 978-0-692-50554-0

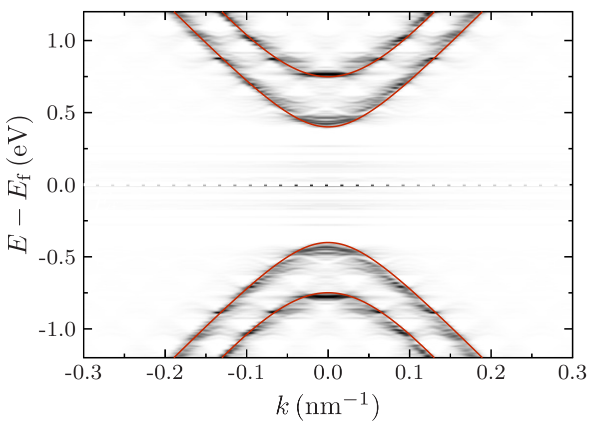

Fig. 1. Atomistically calculated band structure of a (14,0) tube with (grey contour plot) and without (red lines) 5 defects.

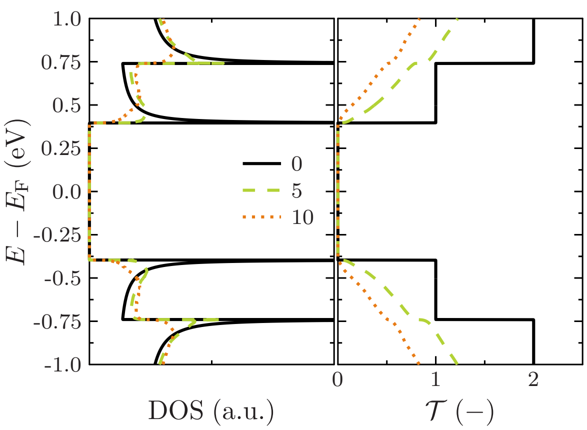

Fig. 2. Atomistically calculated average DOS and transmission spectrum $\mathcal{T}$ of a (14,0) CNT with 0, 5 and 10 defects

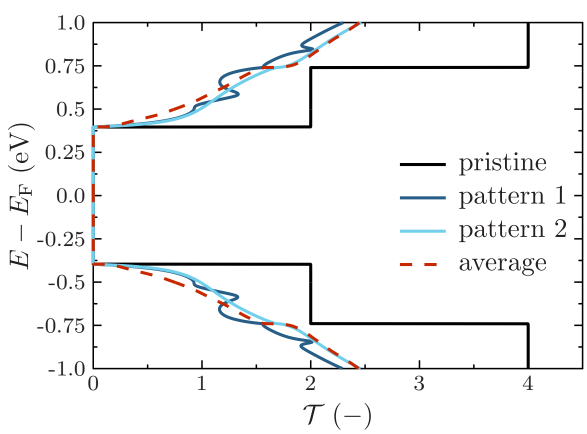

Fig. 3. Atomistically calculated transmission spectra $\mathcal{T}$ for 0 and 3 defects for different arbitrary defect pattern and the average for 100 arbitrary defect pattern.

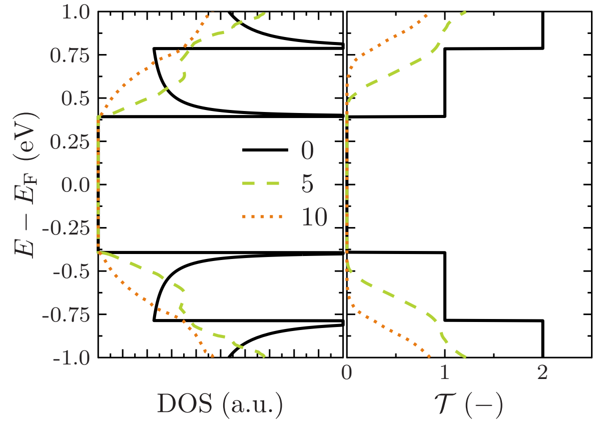

Fig. 4. Local DOS averaged along the channel and transmission spectra for different number of defects calculated at the device level.

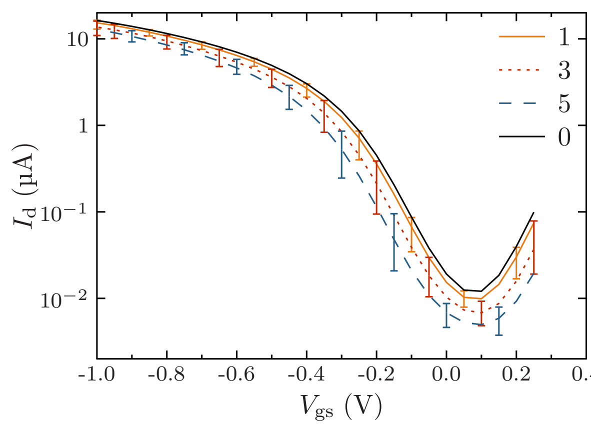

Fig. 5. Averaged transfer characteristic for different number of defects. The error bars indicate the variability of the transfer curves with respect to different defect pattern.

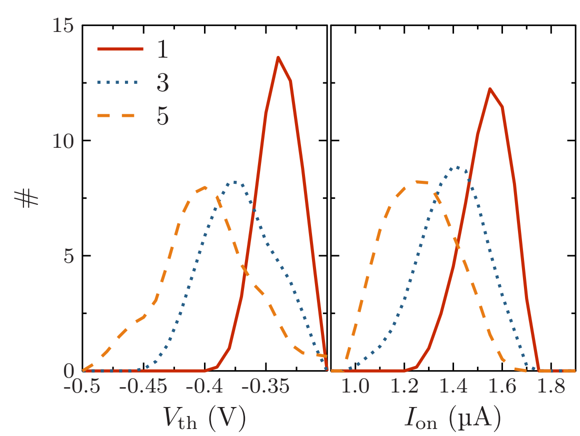

Fig. 6. Distribution of V_{th} and I_{on} for different number of defects randomly distributed along the channel.